Unsteady Nature of Shock-Wave/Turbulent Boundary-Layer Interaction

Kin-Choong Muck,* Jannis Andreopoulos,† and Jean-Paul Dussauge‡
Princeton University, Princeton, New Jersey

This study addresses the unsteady aspect of shock-wave/turbulent boundary-layer interaction. The interaction was generated using a two-dimensional compression ramp at a freestream Mach number of 2.9. Three models were tested, with flow conditions ranging from fully separated to incipient separation. An array of flush-mounted, miniature, high-frequency pressure transducers was used to make multichannel measurements of the fluctuating wall pressure within the interaction. The present results show that, upstream of the mean separation line, the flow is dominated by the large-scale "flapping" motions of a single sharp shock wave. Instantaneously, this shock front is considerably spanwise nonuniform, giving it a "rippling" appearance. In the separated region, however, convective turbulence phenomena play a much larger role. The energy containing turbulent eddies above the recirculation zone and traveling in the downstream direction appear to be the major contributors to the wall pressure fluctuations. Here, the time scale of the pressure signals is found to decrease significantly as the shock strength is increased.

Nomenclature

M = local Mach number
P_w = mean wall pressure
P_1 = upstream wall pressure level
P_2 = estimated mean wall pressure level just downstream of the shock wave
p_w' = pressure fluctuations
q_e = dynamic pressure
Re = Reynolds number
$R_{pp}(\xi_1,\xi_2,\tau)$ = space-time correlation between two points = $[(1/n)\Sigma^{n_i}{}_{-1} p_{w1}'(x,z,t_i)p_{w2}'(x+\xi_1,z+\xi_2 t_i+\tau)]/(\sigma_{pw1}\sigma_{pw2})$
U = local velocity
U_c = convection velocity
u_τ = friction velocity
x = streamwise distance from corner model apex
z = spanwise distance from the tunnel centerline
γ = intermittency factor
δ = boundary-layer thickness
δ^* = displacement thickness
θ = momentum thickness
ξ_1 = separation distance between two transducers in the x direction
ξ_2 = separation distance between two transducers in the z direction
σ_w = rms of pressure fluctuations
τ = time delay
τ_{opt} = optimum time delay for maximum pressure correlation
τ_w = wall shear stress (from Preston tube measurement)

Subscript

0 = incoming undisturbed condition

Introduction

THE behavior of the shock-wave motion and its interaction with a turbulent shear flow is of great practical interest and has been the subject of considerable research in the past. Even so, our present understanding of these complex flows is rather limited and many physical aspects are not well understood. The unsteadiness of the shock wave, particularly when the flow is separated, is one of the little known characteristics in shock-wave/boundary-layer interaction. Such unsteadiness as manifested in the large-scale oscillations of the shock wave can have important practical implications on local heat-transfer rates, noise generation, and aerodynamic loading on high-speed aircraft structures. Current calculation methods are largely based on traditional mean flow concepts without taking account of any shock oscillation effects. Since these prediction schemes have ignored an important aspect of the flow, their validity is questionable. The lack of detailed information on the shock unsteadiness has so far hampered the development of more realistic mathematical models. A careful study of this phenomenon is therefore of practical and fundamental value.

Shock-wave/boundary-layer interaction occurs in a variety of high-speed flows, such as over compression ramps and forward-facing steps or past blunt fins and protuberances. Observation of the unsteady character of the interaction was noted by several early workers.[1-4] Kistler[5] was perhaps the first to make fairly detailed high-frequency measurements in an attempt to characterize such unsteadiness in supersonic turbulent boundary layers over a forward-facing step. Later workers[6-8] provided more measurements of the fluctuating wall pressure in the interaction regions of two-dimensional compression ramp flowfields. Their results indicate that the unsteadiness in each flowfield shares some common statistical properties, such as the fact that the spatial scale of the shock oscillations can span a large fraction of the boundary-layer thickness and that the characteristic time scale is significantly larger than the typical large-eddies time scale. These studies clearly established the gross characteristics of the shock-wave unsteadiness, but detailed information on the time-dependent

Received Dec. 22, 1986; revision received June 10, 1987.

*Research Staff, Mechanical and Aerospace Engineering Department (presently with University of Maryland and National Bureau of Standards, Gaithersburg, MD).

†Research Staff and Lecturer, Mechanical and Aerospace Engineering Department (presently with City College of the City University of New York, New York). Member AIAA.

‡Visiting Scientist, Mechanical and Aerospace Engineering Department (presently with University of Aix-Marseille II, Marseille, France). Member AIAA.

nature of the shock structure is still lacking. The present work seeks to fill that need by providing new information through multichannel measurement of the instantaneous wall pressure in the interaction region of a two-dimensional, separated compression ramp flowfield. The characteristics of the shock-wave oscillation are inferred from these surface pressure signals, which are but "signatures" or "footprints" of the flow above the surface. Visual study of the simultaneously recorded four-channel fluctuating wall pressure signals and fairly extensive correlation measurements provided some new insights into the flow. A discussion on the effects of shock strength is also given.

Experimental Apparatus and Techniques

The tests were performed in the Princeton University 203×203 mm high Reynolds number blowdown wind tunnel. The model was mounted on the tunnel floor approximately 107 cm downstream of the nozzel exit plane. The incoming freestream Mach number was nominally 2.9. The stagnation pressure for all tests was $6.8 \times 10\ \mathrm{N \cdot m^{-2}} \pm 1\%$ and the stagnation temperature was $265\ \mathrm{K} + 5\%$, giving a nominal freestream unit Reynolds number of $6.5 \times 10^7 \mathrm{m^{-1}}$. The wall condition was approximately adiabatic.

Three different two-dimensional ramp models of corner angles 24, 20, and 16 deg were used. There was a 2.5 cm gap on either side of the model for passage of the sidewall boundary layers. To further isolate the interaction and to prevent spillage out of the sides, side fences were used (see Fig. 1). The flow for each model was essentially two-dimensional with minor three-dimensional perturbations.[9]

Measurements were made upstream of each corner using a linear array of miniature high-frequency pressure transducers installed in a cylindrical plug. This plug was fitted flush with the tunnel wall and the transducer array could be aligned either in the streamwise or spanwise direction (see Fig. 1). Due to physical limitations, the minimum spacing between adjacent transducers was 5.08 mm. The ramp could be moved relative to the transducers and, over the present range of travel ($\sim$6 cm), δ changed by approximately 0.6 mm, which has a negligible effect on the flowfield.

The transducers used were Kulite (model XCQ-062-25-D) miniature type, each with an active diameter of 0.071 cm. The natural frequency was quoted by the manufacturer to be close to 500 kHz. They were calibrated statically and referenced to vacuum. Shock tube tests have shown that transducers of this type have dynamic calibrations only a few percent lower than those obtained statically.[10]

The outputs from four adjacent transducers were amplified, filtered, and simultaneously sampled and recorded. Sampling frequencies of 100, 50, 20, and 10 kHz/channel were used. A Preston GMAD-1 A/D converter provided 12 bits plus sign, giving 4096 counts in the 0-10 V range. The overall system uncertainty, including noise and quantization error, was estimated to be ± 0.0038 psi. (The mean wall static pressure of the incoming boundary layer was about 3.4 psi.)

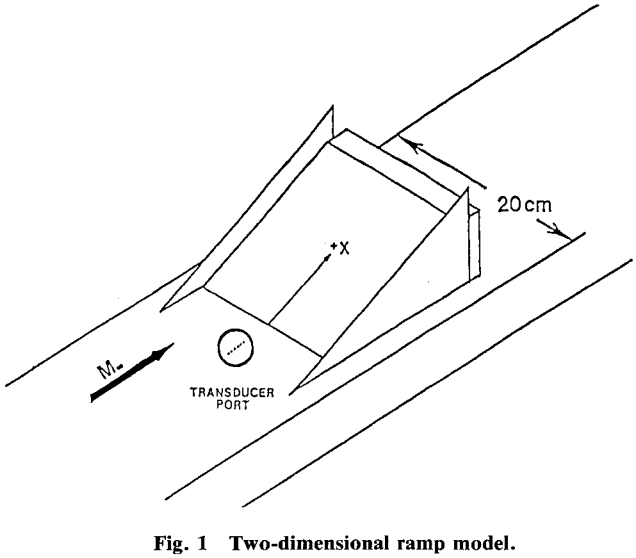

Fig. 1 Two-dimensional ramp model.

Results and Discussion

Incoming Turbulent Boundary Layer

Previous studies using the present wind-tunnel facilities have established that the incoming turbulent boundary layer is essentially two-dimensional and fully developed with zero pressure gradient.[9,11] At the test location, the undisturbed incoming boundary-layer conditions are $M_0 = 2.84 \pm 0.03$, $U_0 = 575 \pm 15\ \mathrm{ms^{-1}}$, $\delta_0 = 24 \pm 2$ mm, $\delta_0{}^* = 6.4 \pm 0.2$ mm, $\theta_0 = 1.3 \pm 0.1$ mm, and $c_{f0} = 0.001 \pm 0.00015$.

In the upstream measuring station, the mean wall pressure, $P_{w0} = 3.4 \pm 0.1$ psi (i.e., $2.4 \times 10^4 \mathrm{N \cdot m^{-2}}$) and the normalized rms wall pressure fluctuations σ_{pw}/P_w was 0.014 ± 0.001 (i.e., $\sigma_{pw}/q_e = 0.0025 \pm 0.0001$, where q_e is the dynamic pressure). Detailed discussion of the repeatability and systematic errors due to spatial resolution have been given previously[12,13] and will not be repeated here.

At the incoming station, $\sigma_{pw}/\tau_w = 2.4$. This value, albeit lower than Kistler and Chan's[14] value, is in good agreement with that found by Speaker and Ailman,[15] Chyu and Hanly,[16] Coe,[6] and Laganelli et al.[17] As reported in previous studies,[8] the probability density distribution of $p_w{}'$ is essentially Gaussian, with skewness and flatness factors of 0.05 and 3.05, respectively.

Figure 2 shows the space-time correlation of the fluctuating wall pressure $R_{pp}(\xi_1/\delta_0, 0, \tau)$ in the incoming boundary layer. The maximum correlation falls with streamwise separation distance, $\xi_1 \cdot R_{pp}(\xi_1/\delta_0, 0, \tau)$, eventually approaches zero at $|\tau| = 0.25$ ms or $|\tau U_0/\delta_0| \simeq 6$ for the different ξ_1 measured. The convection velocity U_c can be estimated from Fig. 2 by dividing the separation distance between the two transducers by the time $\tau_{\max}$, where $\tau_{\max}$ is the time corresponding to maximum R_{pp}. Values for U_c thus obtained are 0.7, 0.7, and 0.75 for $\xi_1/\delta_0 = 0.23$, 0.46, and 0.69, respectively, giving very good agreement with the results of Willmarth and Wooldridge.[18]

The values of the optimum space-time correlation, $R_{pp}(\xi_1/\delta_0, 0, \tau_{\mathrm{opt}})$ are plotted vs the nondimensional transducer separation distance $\xi_1 u_\tau / U_c \delta_0$ in Fig. 3. Here, $\xi_1 u_\tau / U_c \delta_0$ represents the ratio of two time scales, namely, ξ_1/U_c, which is the characteristic convection time of the large eddies, and δ_0/u_τ, which is the time scale of the energy-containing eddies. It can be seen that the present results compare favorably with those of other workers.[15,16,19-21]

Global Flow Features within the Interaction

The mean flowfield of the 24 deg corner model deduced from pitot and static pressure surveys (due to Settles[9]) is shown in Fig. 4. Significant separation occurred about the corner. The flow is first disturbed well upstream of mean separation location (marked I in Fig. 4). The region between the mean separation location and the location at which the mean pressure starts to rise is commonly referred to as the region of "upstream influence" where, from shadowgram pictures, the shock wave is usually observed to be located. One such shadowgram is shown in Fig. 5. The typical "layered" look of the shock front can be seen, giving the impression that a shock fan composed of a series of shock waves exists. Since the shadowgram picture integrates across the span of the flow, it is unclear whether this layered look is due to a shock fan or, indeed the result of spanwise nonuniformity of a single shock wave causing it to ripple. This question will be addressed in the next section.

Figure 6 shows the streamwise distributions of the mean wall pressure P_w ahead of the corner apex for the three models. Only measurements upstream of the corner are presented. The locations of the initial pressure rise and the mean separation are marked "I" and "S" in the figure. The corresponding streamwise distributions of the nondimen-

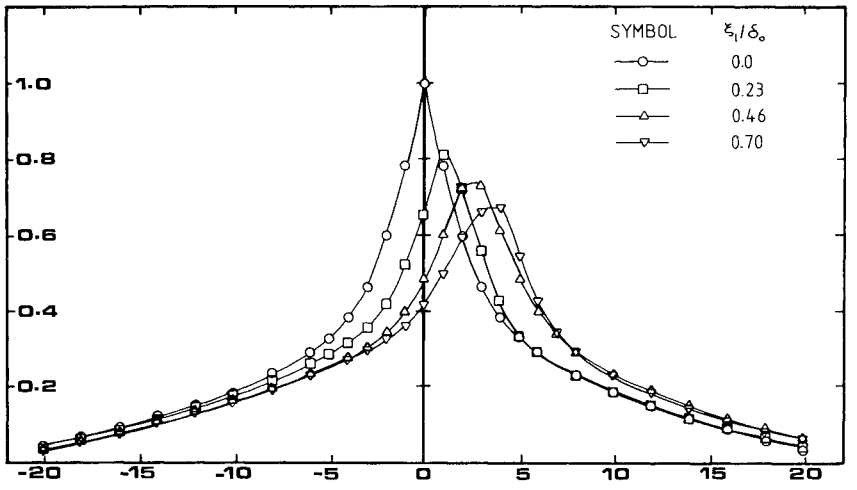

Fig. 2 Streamwise space-time correlations of the pressure fluctuations in the incoming boundary layer.

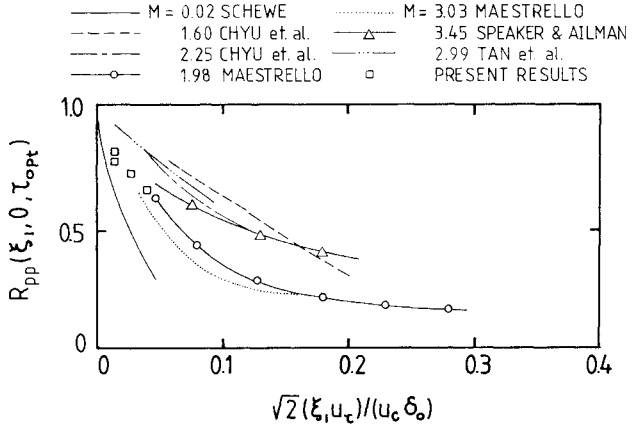

Fig. 3 Optimum space-time correlations of the incoming boundary layer.

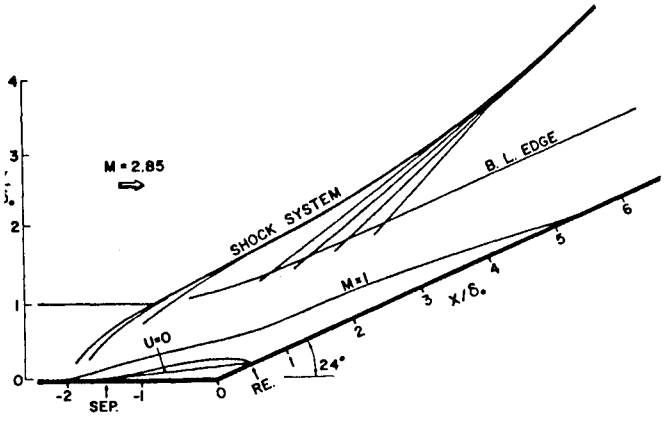

Fig. 4 Sketch of the mean flowfield for the 24 deg model (from Settles et al.[11]).

sionalized rms wall pressure fluctuations σ_{pw}/P_w are shown in Fig. 7. In all cases, the distributions show sharp peaks occurring ahead of the mean separation. For the 24 deg model, σ_{pw}/P_w reaches a maximum value about 15 times its upstream value. Smaller increases are seen for the other two models. The large increase of σ_{pw} is due to the intermittent nature of the pressure fluctuations caused by shock oscillations. We will refer to this region as the "intermittent" region.

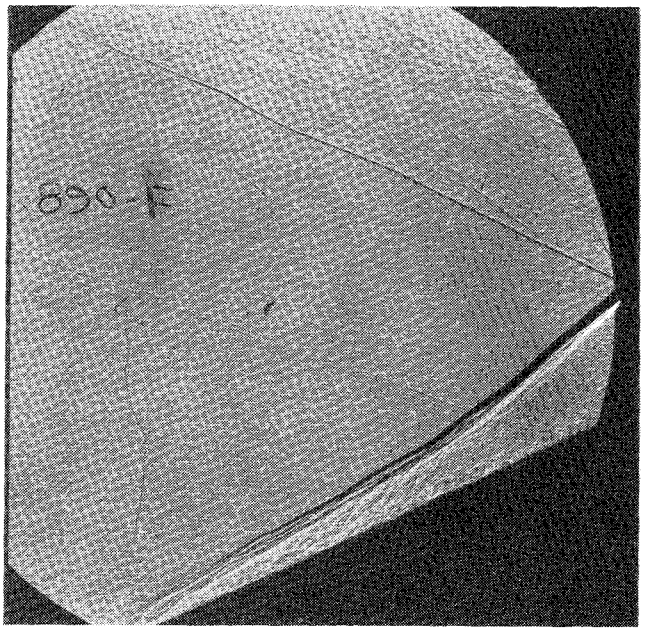

Fig. 5 Shadowgram of the 24 deg model flow.

Instantaneous Shock Structure in the Intermittent Region

Typical streamwise four-channel time-history plots of the fluctuating wall pressure (for the 24 deg model) in the intermittent region are shown in Fig. 8. Those for the 20 and 16 deg models are very similar and will not be shown. These plots clearly indicate the large-scale streamwise oscillatory motion or "flapping" of the shock wave. The signals are highly intermittent and appear to jump back and forth between two levels, which are the upstream level indicated by P_1 and the "high" level marked P_2 in the figures. P_2 is presumably the level measured when the "foot" of the shock wave was upstream of the transducer and vice versa, while P_1 was measured when the shock was downstream of the transducer. A number of small spikes are also seen in the figures; these were probably measured when the foot of the shock was just touching the transducer.

The pressure difference between the upstream and the "high" levels, $\Delta P = P_2/P_1$, is about 1.7 on average. Referring to Fig. 2, the pressure rise to separation is very close to 1.7 for all three models. In view of the intermittent nature of the pressure signal, one can conveniently model it as a "boxcar" signal, which in fact was first suggested by Kistler.[5] The mean wall pressure in this region is then made up of contributions

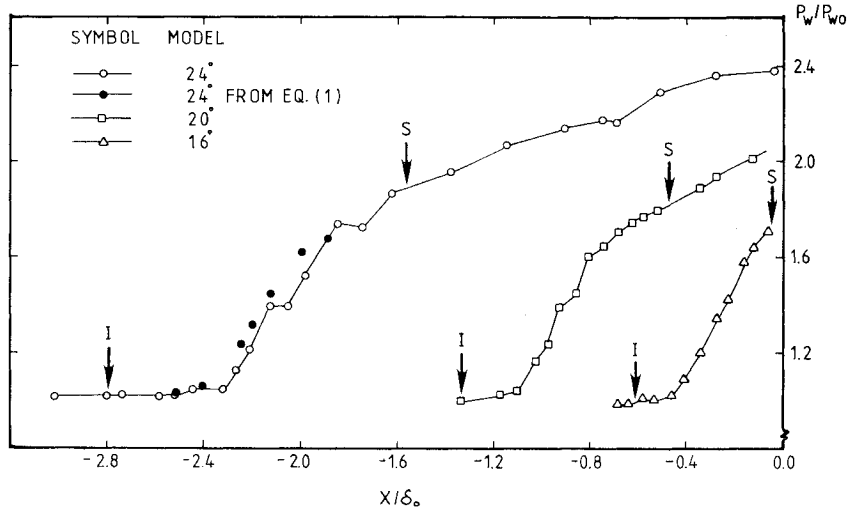

Fig. 6 Longitudinal mean pressure distributions within the interaction.

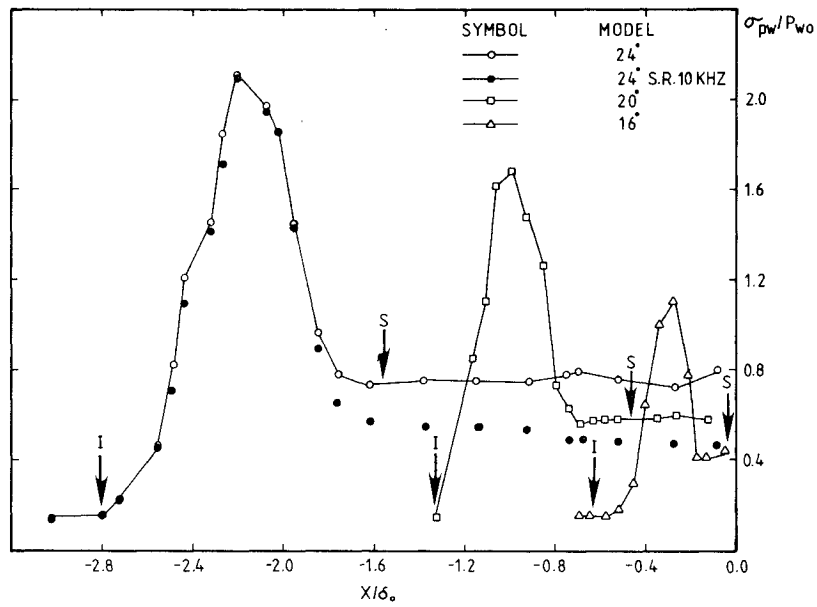

Fig. 7 Longitudinal distributions of rms pressure fluctuation σ_{pw} (sampling rate was 100 kHz/channel, unless stated otherwise).

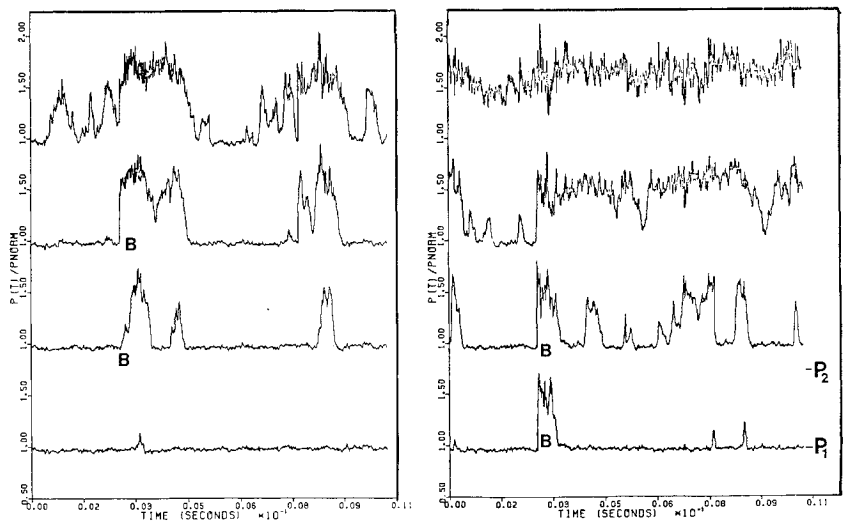

Fig. 8 Time-history plots of the simultaneously recorded four-channel (streamwise) fluctuating wall pressure in the intermittent region for the 24 deg model.

from the low level P_{w0} ($=P_1$) and the high level P_2 according to

$$P_w = (1-\gamma)P_1 + \gamma P_2 \quad (1)$$

where γ is the intermittency factor defined as the average fraction of the time at a point when the shock wave is upstream of the transducer. In this case, γ varies from 0 when the flow is first disturbed to 1.0 at the mean separation point. Measurement of γ in the present flow was previously reported by Dolling and Or[8], and Andreopoulos and Muck[22], and will not be repeated here. ΔP is set equal to 1.7. The streamwise distribution of P_w evaluated according to Eq. (1) is shown in Fig. 6 for the 24 deg model in this region.

It is worth pointing out that the pressure rise across the shock is only 1.7, although the total pressure rise is close to 4.1 for the 24 deg model.[11] Based on invicid theory, for a freestream Mach number of 2.9 and a pressure ratio of 1.7, the flow turning is about 7 deg. Settles et al.[11] reported that the present flow, indeed, first turns through only 10 deg at the initial part of the interaction, while the other 14 deg of the total turning is effected more gradually downstream.

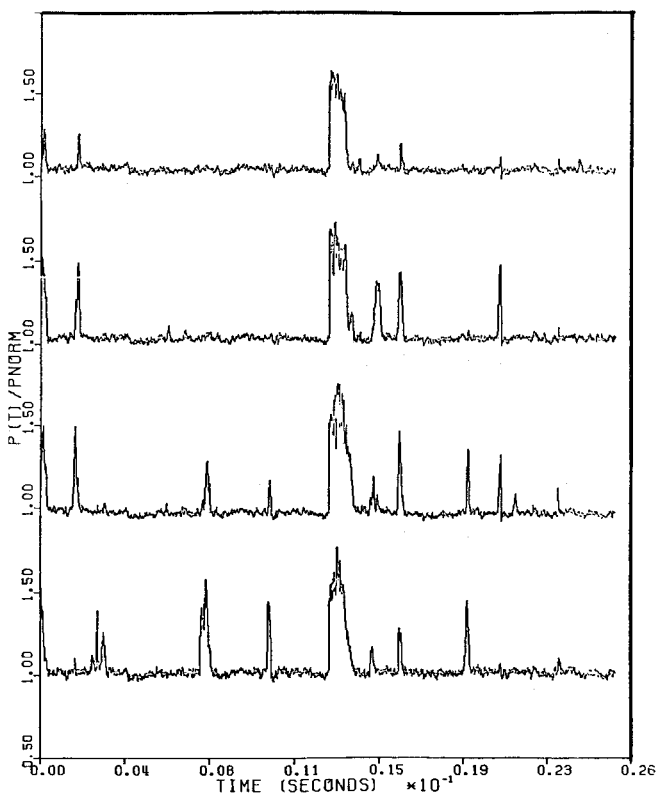

Fig. 9 Time-history plots of the simultaneously recorded four-channel (spanwise) fluctuating wall pressure in the intermittent region for the 24 deg model.

The layered look of the shock wave as seen in the shadowgram raised some questions about its interpretation, since either spanwise shock rippling or a shock fan can produce the same appearance. If a shock fan were to exist, then one would expect to see significant variations in the wall pressure with the streamwise distance. The pressure fluctuations after the shock (see, for example, the portions marked "B" in Fig. 8) measured by successive transducers simultaneously are relatively little changed over a significant distance ($\delta \geq 0.5$). This observation suggests that the instantaneous shock structure in the intermittent region is essentially a single sharp shock wave that flaps back and forth with a streamwise length scale of the order of δ. The layered appearance alluded to earlier is then not likely to be caused by a shock fan, but due to spanwise rippling of the shock wave.

Evidence of rippling can be seen in Fig. 9, which shows the four-channel recording of the wall pressure with the transducer array aligned in the spanwise direction for the 24 deg model. Measurements at only one streamwise location ($x/\delta_0 = -2.41$) are shown. This figure clearly shows that the shock front is not two-dimensional, but can exhibit significant spanwise ripples. These ripples had wavelengths as small as (if not smaller than) $\xi_2/\delta_0 = 0.23$ and as large as (if not larger than) $\xi_2/\delta_0 = 0.69$. This is the first direct evidence of shock rippling. It should be noted that shock "rippling" is not synonymous with shock "flapping"; the latter describes the streamwise motion of the shock, while the former is a description of the appearance of the shock front.

By visual inspection of the time-history traces, the shock wave is observed to exhibit the same degree of spanwise rippling for all three models. We note that there is a large difference between the 24 deg model flow, which has a large separation region, and that of the 16 deg model flow, which is experiencing only incipient separation. Since the incoming boundary layer is the same in both cases, one is led to infer that the incoming turbulent structures are intimately related to the shock ripplings. Andreopoulos and Muck[22] recently suggested that the large turbulent eddies are a strong contender as the mechanism causing shock oscillations. Their proposal is consistent with the present observation and supports the belief that the turbulent eddies are a likely cause of shock rippling.

Pressure Correlation Measurements

Figure 10 shows the autocorrelations of the wall pressure at different locations within the interaction for the 24 deg model. In the region where the pressure signals are highly intermit-

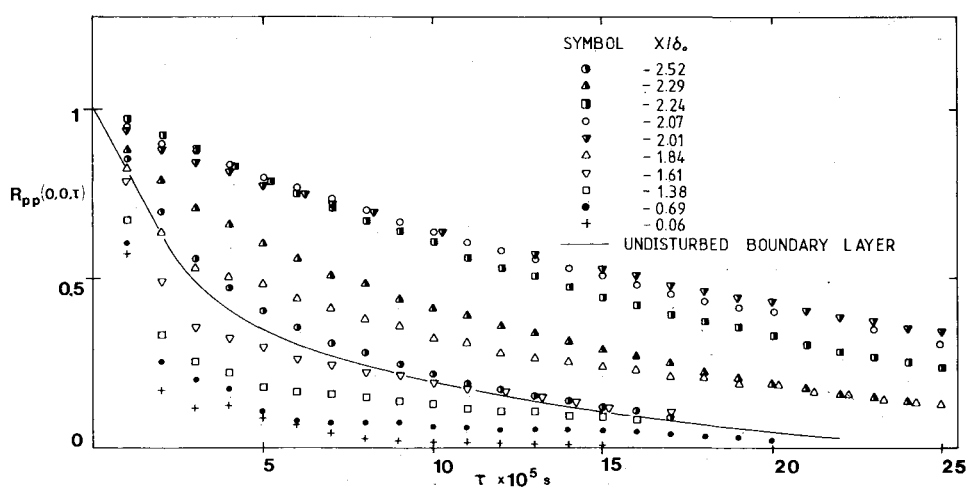

Fig. 10 Autocorrelation of the pressure fluctuations of the 24 deg model.

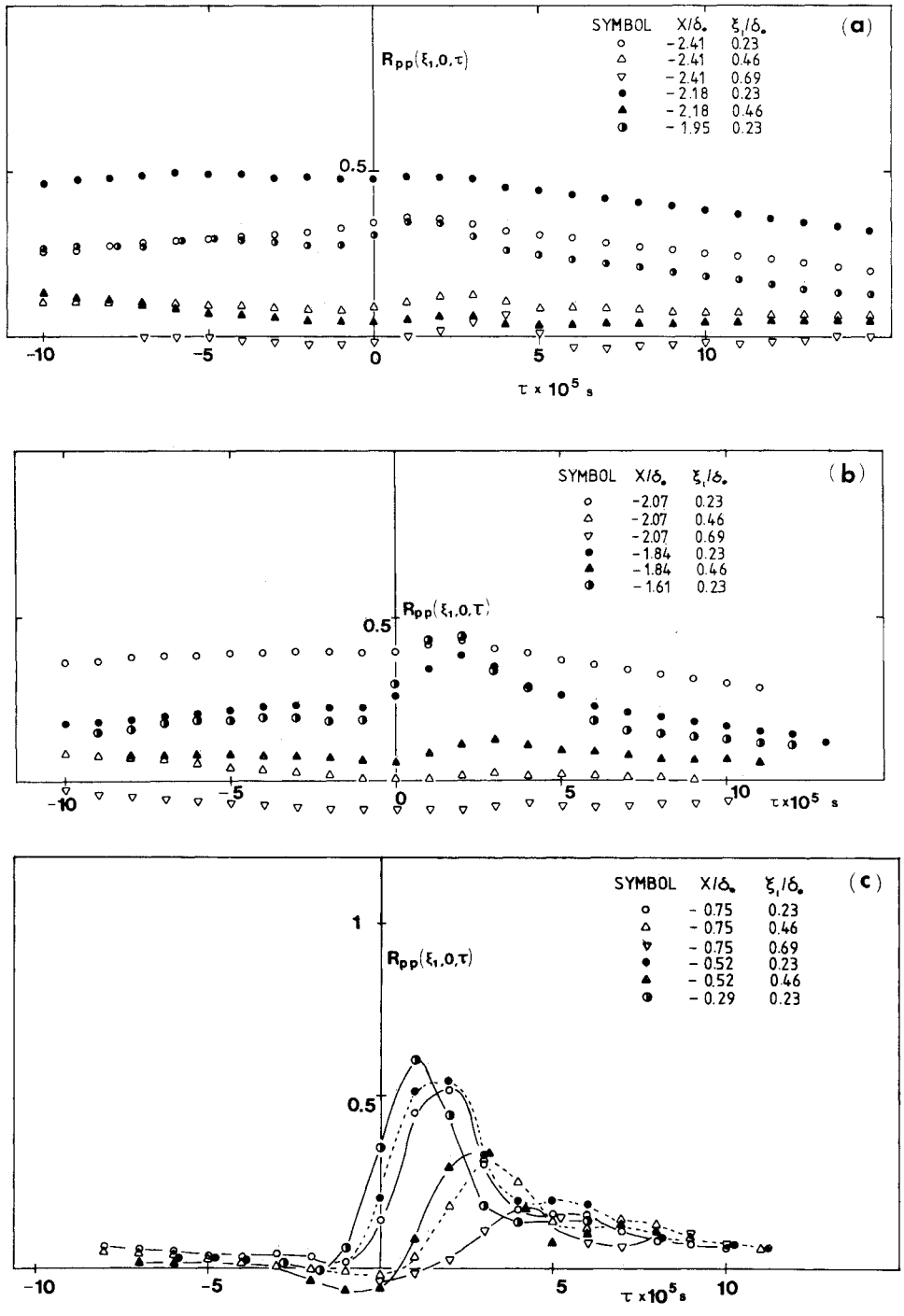

Fig. 11 Space-time correlations in the 24 deg model flowfield.

tent, the autocorrelation reaches values much higher than those in the undisturbed boundary layer. The autocorrelation remains high for a large range of delay time τ, which suggests that large-scale in-phased motions are predominant. The largest correlation is found in the region $-2.24 \leq x/\delta_0 \leq -2.0$ where the intermittency is about 0.5. Evidently, the high correlations are closely related to the shock wave oscillating back and forth over the transducers. The autocorrelation is seen to decrease further downstream. Beyond the mean separation location, it even falls below the upstream value. In fact, the lowest correlation was measured at $x/\delta_0 \simeq -0.06$ (which is very close to the corner apex). The low autocorrelation in the region close to the corner is indicative of the predominance of eddies of high characteristic frequencies in the separated region of the flow.

Longitudinal space-time correlations were also measured at various locations inside the interaction region, including the separation region. These are plotted in Fig. 11. Figures 11a and 11b show the space-time correlations obtained at locations upstream of the mean separation location, while Fig. 11c shows those in the separated region. Comparing Fig. 11 to Fig. 2, it is seen that the space-time correlation behavior of the flow in the interaction region is drastically different from that in the upstream undisturbed boundary layer. The upstream pressure fluctuations are associated with turbulent convective phenomena in the direction of the flow. In the intermittent region, however, the flow is dominated by large-scale oscillating motions, with convective turbulence playing only a minor role. Inside the separation region, the space-time correlation is even more complicated. The pressure field is af-

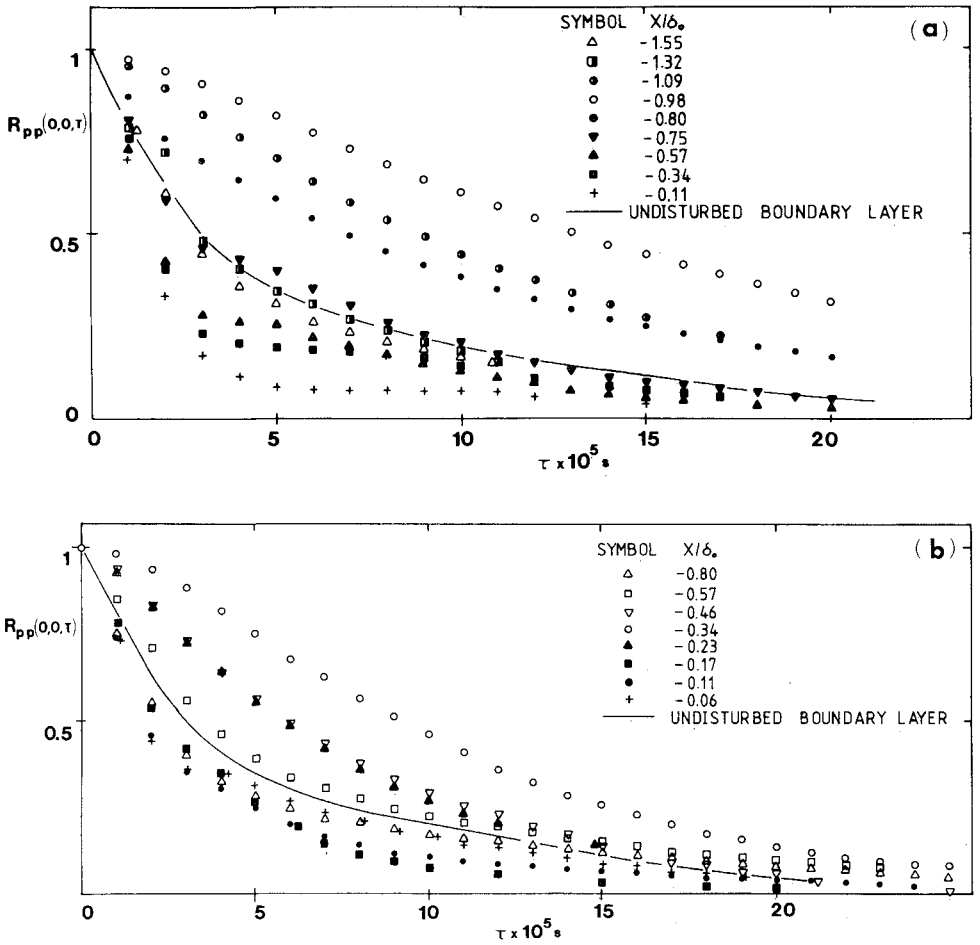

Fig. 12 Autocorrelations of the pressure fluctuation in the 20 and 16 deg model flows.

fected by the large turbulent structures moving in the direction of the external flow and also by those structures close to the wall moving in the opposite direction, in addition to any residual effects of the shock oscillation.

In Fig. 11a, the peak value of the space-time correlation R_{pp} at the start of the interaction at $x/\delta_0 = -2.41$ and for $\xi_1/\delta_0 = 0.23$ is about 0.37. This is considerably lower than that in the upstream boundary layer, where the corresponding value is about 0.8. But just further downstream at $x/\delta_0 = -2.18$, the peak value of R_{pp} jumps to about 0.5 (for $\xi_1 = 0.23$). This location corresponds to the mean location of the unsteady shock, where σ_{pw} is at a maximum. Here, the oscillatory behavior of the shock wave is believed to contribute to the jump in R_{pp}. Evidently, the same phenomenon is also responsible for the rather "flat-top" behavior of R_{pp} about the small delay time. A flat-top behavior can be interpreted in terms of large-scale, in-phased motion or very high convection velocity.

Referring to Fig. 11b, negative R_{pp} is seen at $x/\delta_0 = -2.07$ when the separation distance ξ_1 is 0.69. For such large ξ_1, the downstream transducer is, in fact, located inside the separated region. This negative correlation is likely to be caused by out-of-phase fluctuations of the shock wave between the two measuring points.

Also observed in Fig. 11b is the development of sharp peaks in R_{pp} (for $\xi_1 = 0.23$) further downstream for positive delay time. This behavior is more pronounced inside the separated region, as can be seen in Fig. 11c. Here, the maximum correlation at positive τ, albeit significantly below the upstream value, increases with downstream distance, while the maximum at negative τ practically disappears. A likely explanation of this behavior is that, as the flow progresses further into the interaction, the direct effect of the shock oscillations is diminished so that the flow is once again dominated by the convective behavior of turbulent eddies. In fact, the convection velocities calculated from the peak values at positive τ for various separations ξ_1/δ_0 are roughly the same within the temporal resolution of the present experiment (which is of order 10 μs). Coupled with a lack of appreciable peak at negative τ, this behavior suggests that the large eddies at the top of the separation bubble moving in the external flow direction are the major contributors to the wall pressure fluctuations.

Effects of Shock Strength

The results for the other two corners with angles 20 and 16 deg show that there are qualitative and quantitative differences from those of the 24 deg corner. As was previously reported by Settles,[9] the 16 deg corner flowfield is just separated with a very small separation bubble at the corner (i.e., incipient separation condition), while for the 20 and 24 deg cases, the flow is fully separated. The shock strength as characterized by the pressure increase across the shock wave is, of course, increasing with increasing corner angle. In this experiment, the incoming boundary layer was the same for all three models.

Figure 12 shows the autocorrelation curves for the 20 and the 16 deg models. These figures are to be compared to Fig. 10 showing the same for the 24 deg model. At the beginning of the interaction, the autocorrelation is increased significantly due to the shock oscillations in each case. Comparing the lowest measured autocorrelation for the three models provided an interesting observation. In all cases, the lowest values are found at stations close to the apex. It can be seen that the 24 deg model case exhibits the sharpest fall-off at small τ. This behavior is, however, less pronounced as the shock strength is reduced, suggesting that the turbulence microscales and integral scales as inferred from the wall pressure fluctuations inside the separated region increase with decreasing corner angle. These scales are effectively time scales rather than

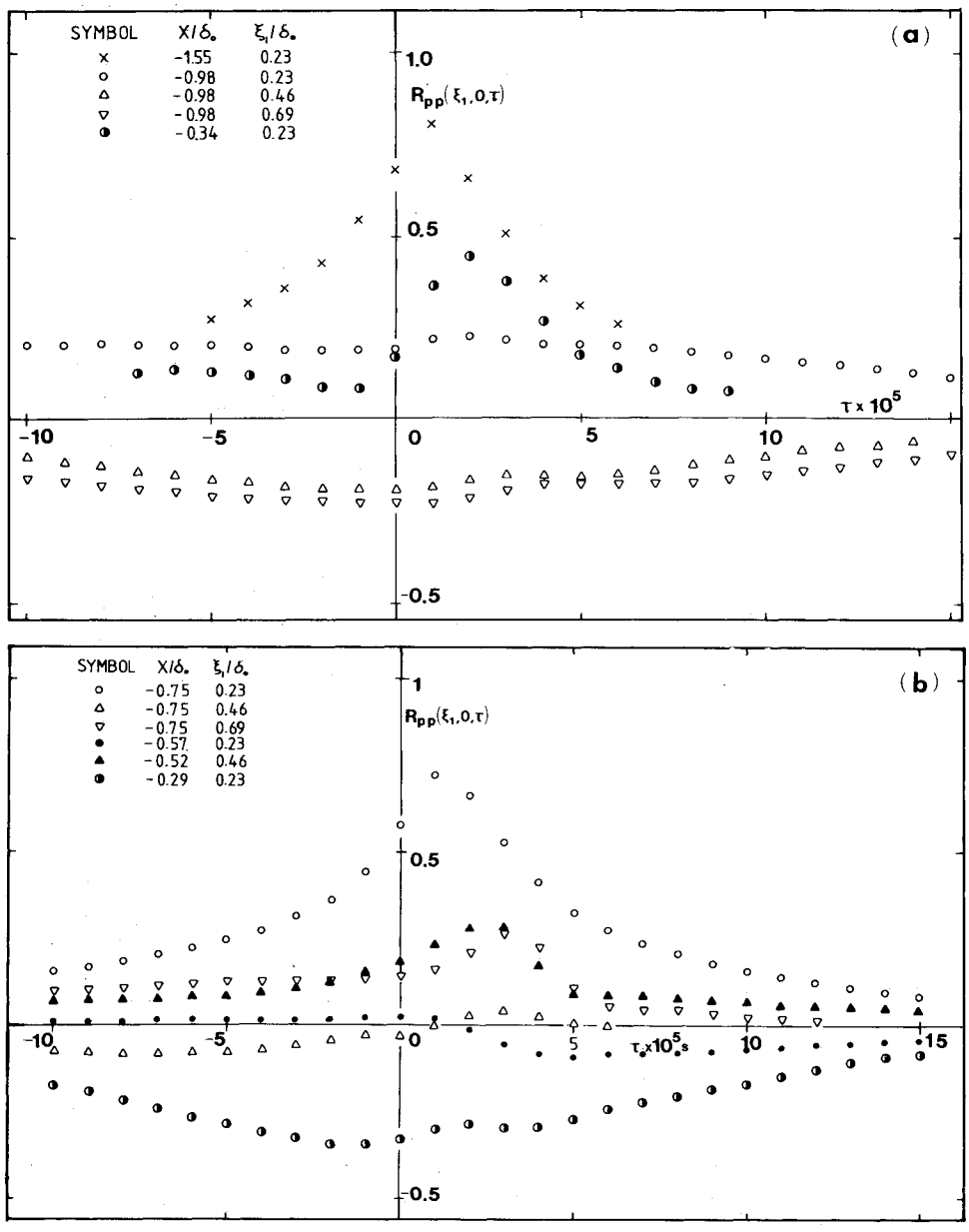

Fig. 13 Space-time correlations in the 20 and 16 deg model flows.

length scales and, therefore, indicate the shift in the frequency contents with decreasing angle.

Figure 13 shows the streamwise space-time correlation at different stations for the 20 and 16 deg models. Even more pronounced negative correlations are seen, compared to the 24 deg model. It should be remembered that, for the smaller-angle models, the intermittent region and mean separation location are formed closer to the apex. The rather considerable negative correlations seen in the figures are expected to be due to out-of-phase fluctuations of the shock wave at those measuring points. Further into the interaction, rather sharp peaks appear in the correlations. This allows the convection velocity U_c to be estimated. The U_c/U_0 found for the 24 and 20 deg models in the separated zone are 0.60 and 0.48, respectively. (It is not possible to estimate U_c for the 16 deg model because even the most downstream data did not produce any distinct peak. The reader is reminded that the convection velocity in the undisturbed boundary layer is about 0.7 (given above). Those given here are indicative of a flow still undergoing distortion through the interaction. But it is clear that the convection velocity in the separated region is significantly reduced. It is also interesting to note that U_c drops with decreasing shock strength. This behavior is evidently the result of the decrease in the time scale with increasing shock strength in this region alluded to earlier, without a corresponding decrease in the length scale.[23]

Conclusions

The unsteady aspect of compression ramp generated shock-wave/turbulent boundary-layer interaction is studied. Three two-dimensional models were used, giving flow conditions ranging from fully separated to incipient separation. An extensive data set obtained from simultaneous multichannel high-frequency recordings of the fluctuating wall pressure provided some new information on this little-known phenomenon.

Throughout the interaction, the flow is affected by two basically different phenomena, namely, the flapping motions of the shock wave and convective turbulence effects. Their relative importance, however, is strongly dependent on the location within the interaction. In the region just upstream of mean separation, where the pressure signals are intermittent, the flow is dominated by the large-scale oscillations of essen-

tially a single sharp shock wave. This shock wave is significantly three-dimensional, showing spanwise rippling. The incoming turbulent eddies convected into the interaction are believed to be causing these spanwise ripples.

In the separated region, a much larger contribution from the high-frequency fluctuations is evident. Turbulent transport phenomenon predominates over the oscillatory motions. The energy-containing eddies above the flow recirculation zone traveling in the downstream direction seem to be the major contributors to the wall pressure. Here, a marked decrease in the time scale is found, particularly with increasing shock strength, leading to a significant drop in the convection velocity.

Acknowledgments

This work was supported by U.S. Air Force Office of Scientific Research Grant 85-1026 and AFOSR Contract F49620-84-C-0086, monitored by Drs. J. McMichael and J. Wilson. One of the authors, J.P. Dussauge, was supported by a bourse de voyage de l'OTAN, which is gratefully acknowledged. The authors would like to acknowledge stimulating discussions with Profs. A.J. Smits and S.M. Bogdonoff. The authors also thank Mr. Tak Or for his help with measurements.

References

[1]Bogdonoff, S.M., "Some Experimental Studies of the Separation of Supersonic Turbulent Boundary Layers," Dept. of Aeronautical Engineering, Princeton University, Princeton, NJ, Rept. 336, June 1955.

[2]Price, A.E. and Stalling, R.L., "Investigation of Turbulent Separated Flows in the Vicinity of Fin Type Protuberances at Supersonic Mach Numbers," NASA TN D-3840, 1967.

[3]Kaufman, L.G., Korkegi, R.H., and Morton, L., "Shock Impingement Caused by Boundary Layer Separation Ahead of Blunt Fins," ARL 72-0118, 1972.

[4]Winkelman, A.E., "Experimental Investigation of a Fin Protuberance Partially Immersed in a Turbulent Boundary Layer at Mach 5," NOLTR-72-33, Jan. 1972.

[5]Kistler, A.L., "Fluctuating Wall Pressure Under a Separated Supersonic Flow," *Journal of the Acoustical Society of America,* Vol. 36, March 1964, pp. 543–550.

[6]Coe, C.F., "Surface-Pressure Fluctuations Associated with Aerodynamic Noise," NASA SP-207, 1969, pp. 409–424.

[7]Dolling, D.S. and Murphy, M., "Wall Pressure Fluctuations in a Supersonic Separated Compression Ramp Flowfield," AIAA Paper 82-0986, June 1982.

[8]Dolling, D.S. and Or, T.C., "Unsteadiness of the Shock Wave Structure in Attached and Separated Compression Ramp Flowfields," AIAA Paper 83-1715, July 1983.

[9]Settles, G.S., "An Experimental Study of Compressible Turbulent Boundary Layer Separation at High Reynolds Numbers," Ph.D. Dissertation, Aerospace and Mechanical Engineering Dept., Princeton University, Princeton, NJ, Sept. 1975.

[10]Raman, K.R., "A Study of Surface Pressure Fluctuations in Hypersonic Turbulent Boundary Layers," NASA CR-2386, Feb. 1974.

[11]Settles, G.S., Vas, I.E., and Bogdonoff, S.M., "Details of a Shock Separated Turbulent Boundary Layer at a Compression Corner," *AIAA Journal,* Vol. 14, Dec. 1976, p. 1709.

[12]Muck, K.C., Dussauge, J.P., and Bogdonoff, S.M., "Structure of the Wall Pressure Fluctuations in a Shock-Induced Separated Turbulent Flow," AIAA Paper 85-0179, Jan. 1985.

[13]Dussauge, J.P., Muck, K.C., and Andreopoulos, J., "Properties of Wall Pressure Fluctuations in a Separated Flow Over a Compression Ramp," IUTAM Symposium on Turbulent Shear Layer/Shock Wave Interaction, Palaiseau, France, edited by J. Dēlery, Springer-Verlag, Berlin, 1986, p. 383.

[14]Kistler, A.L. and Chen, W.S., "The Fluctuating Pressure Field in a Supersonic Turbulent Boundary Layer," *Journal of Fluid Mechanics,* Vol. 16, 1963, p. 41.

[15]Speaker, W.V. and Ailman, C.M., "Spectra and Space-Time Correlations of the Fluctuating Pressures at a Wall Beneath a Supersonic Turbulent Boundary Layer Perturbed by Steps and Shock Waves," NASA CR-486, 1966.

[16]Chuy, W.J. and Hanly, R.D., "Power and Cross Spectra and Space-Time Correlations of Surface Fluctuating Pressures at Mach Numbers Between 1.6 and 2.5," AIAA Paper 68-77, Jan. 1968.

[17]Laganelli, A.L., Martellucci, A. and Shaw, L.L., "Wall Pressure Fluctuations in Attached Boundary Layer Flow," *AIAA Journal,* Vol. 21, April 1983, p. 495.

[18]Willmarth, W.W. and Wooldridge, C.E., "Measurements of the Fluctuating Pressure at the Wall beneath a Thick Turbulent Boundary Layer," *Journal of Fluid Mechanics,* Vol. 14, 1962, p. 187.

[19]Schewe, G., "On the Structure and Resolution of Wall-Pressure Fluctuations Associated with Turbulent Boundary-Layer Flow," *Journal of Fluid Mechanics,* Vol. 134, 1983, pp. 311–328.

[20]Maestrello, L., "Radiation from and Panel Response to a Supersonic Turbulent Boundary Layer," Boing Scientific Research Laboratories, Doc. D1-82-0719, Sept. 1968.

[21]Tan, D.K.M., Tran, T.T., and Bogdonoff, S.M., "Wall Pressure Fluctuations in a Three-Dimensional Shock Wave/Turbulent Boundary Layer Interaction," *AIAA Journal,* Vol. 25, Jan. 1987, p. 14.

[22]Andreopoulos, J. and Muck, K.C., "Some New Aspects of the Shock Wave Boundary Layer Interaction in Compression Ramp Flows," *Journal of Fluid Mechanics*, Vol. 180, 1987, pp. 405–428.

[23]Smits, A.J. and Muck, K.C., "Experimental Study of Three Shock Wave/Turbulent Boundary Layer Interactions," (to be published in *Journal of Fluid Mechanics*).